LOOP MODELS FROM SOHO OBSERVATIONS

M. Landini[1], A. Brković [2], E. Landi[1,3], I. Rüedi[2], S. Solanki[2]

[1] Dipartimento di Astronomia e Scienza dello Spazio, Università di Firenze, Italy
[2] Institute of Astronomy, ETH-Zentrum, Switzerland
[3] Max-Planck-Institute für Aeronomie, Katlenburg-Lindau, Germany

ABSTRACT

In the present work CDS,EIT,MDI and Yohkoh observations of active region loops have been analyzed. These observations are part of JOP 54. CDS monochromatic images from lines at different temperatures have been co-aligned with EIT and MDI images and loop structures have been clearly identified using Fe XVI emission lines. Density sensitive lines and lines from adjacent stages of ionization of Fe ions have been used to measure electron density and temperature along the loop length; these measurements have been used to determine the electron pressure along the loop and to test the constant pressure assumption commonly used in loop modeling. The observations have been compared with a static, isobaric loop model assuming a temperature-constant heating function in the energy balance equation and variable loop section. Good agreement is found between model and observations. Comparison is also made between temperature and pressure model predictions and direct measurements using line ratios.

1. INTRODUCTION

The first attempts to model loop structures of the solar corona date back to the 1970s in connection with the large number of broad band x-ray pictures obtained by Skylab. One of the first models was published by one of the authors with the aim to predict x-ray emission from stellar coronae (Landini & Monsignori Fossi 1973) and successively developed to allow comparison with solar observations (Landini & Monsignori Fossi 1975). The model was based on the solution of the energy balance among radiative losses energy input and conductive energy in a constant-section, stationary and static loop.

A few years later Rosner *et al.* (1978, from now on RTV) improved that model using a better approximation to the radiative losses versus temperature function and investigating different mechanisms of power supply. Extensive use has been made in the last twenty years of the RTV scale length that has been applied to coronal loop observations from SMM to Yohkoh and the model itself has been extended to include velocity fields and the effect of gravity (Peres 1997).

Most of the solar missions devoted to the study of the solar corona launched in the last twenty years have produced increasingly better spatially resolved images of the solar corona with rather poor spectral resolution, using broad band detectors. This has not allowed a detailed temperature and density diagnostic of single loops in order to investigate model predictions from the transition region to the hot corona. The coronal instruments on SOHO, in particular CDS and SUMER, have the ability to image selected regions of the solar corona using monochromatic light over a very wide spectral region of the EUV spectral range. A number of high spatial and spectral resolution maps are now available to study in detail many coronal structures.

The aim of this paper is to extend the loop model originally developed in 1975 and to compare its predictions with observations obtained with the Coronal Diagnostic Spectrometer (CDS) on board SOHO (Harrison *et al.* 1995). A set of 19 simultaneous CDS monochromatic images of a complex loops structure is used, a diagnostic technique discussed in the text is applied to some loops found in the active region. Electron temperature and density models along the loops are discussed and compared with line-ratio results from CDS, and the necessary power supply is evaluated.

2. THE OBSERVATION

The observations were taken on April 29^{th} 1997, between 8:20 and 10:40 AM, on an active region on the solar disk centered at around (-100",-400") in heliocentric coordinates.

The CDS observations consist of several spectral windows taken around selected wavelengths, in order to observe both transition region and coronal lines. The observed lines come from the Chromosphere (He I), the Transition Region (O III, O V, Ne V, Mg VII) and the Corona (Mg VIII, Mg IX, Si XI, Si XII, Fe XII, Fe XIII, Fe XIV, Fe XVI). These lines allow density diagnostics using Fe XII and Fe XIII lines and sample the plasma up to temperatures around 2.5×10^6 K. The presence of consecutive stages of ionization for several elements allows temperature diagnostics through intensity ratios of lines of different

Proceedings 8th SOHO Workshop 'Plasma Dynamics and Diagnostics in the Solar Transition Region and Corona', Paris, France, 22-25 June 1999, (ESA SP-446, October 1999)

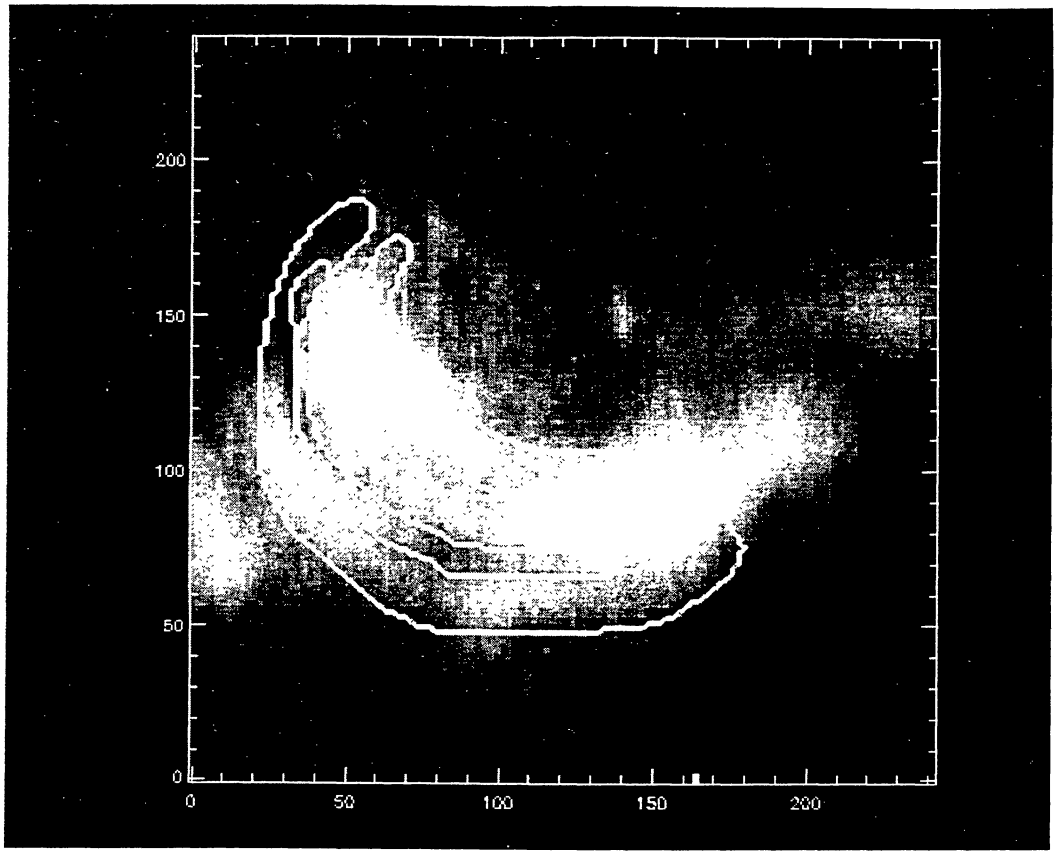

Figure 1. Intensity map of the Fe XVI 335.4 Å line with adopted loop contours. The loops are numbered as follows: 1 refers to the outermost structure, 2 to the middle structure and 3 to the innermost, shortest structure in the map.

ions. The observations have been co-aligned using a cross-correlation technique with EIT and Yohkoh full-disk images. Loop structures (in particular their footpoints) have been identified also with the help of MDI magnetograms.

The list of used lines is given in Table 1.

Theoretical intensity ratios for density and temperature diagnostics have been calculated using the CHIANTI database (Dere *et al.* 1997, Landi *et al.* 1998).

3. DATA ANALYSIS

3.1. Morphology of the emitting region

The hottest emitting plasma is confined in few loop-like regions whose footpoints correspond to photospheric enhancements of magnetic field of opposite polarity (Fig. 2). The shape of the loops is evident with Fe XVI lines (Fig. 1), revealing the presence of three distinct structures. The loop contours are overplotted in Fig. 1. The outlines were determined after comparing with the emission from different ionization stages of iron, which showed maximum brightness in different parts of the loops.
Each loop has been divided in many sections, in or-

Ion	λ (Å)	Log T	Detector
Si VIII	314.327	5.93	NIS 1
Mg VIII	315.039	5.91	NIS 1
Fe XIII	318.128	6.20	NIS 1
Fe XIV	334.172	6.27	NIS 1
Fe XVI	335.410	6.43	NIS 1
Fe XII	338.278	6.14	NIS 1
Fe XIII	348.183	6.20	NIS 1
Ne V	359.382	5.47	NIS 1
Fe XIII	359.642	6.20	NIS 1
	359.842	6.20	NIS 1
Fe XVI	360.760	6.43	NIS 1
Fe XII	364.467	6.14	NIS 1
Mg VII	367.674	5.81	NIS 1
	367.683	5.81	NIS 1
Mg IX	368.070	5.98	NIS 1
Si XII	520.665	6.27	NIS 2
Si XI	580.907	6.20	NIS 2
He I	584.334	4.00	NIS 2
O III	599.597	4.96	NIS 2
Si XI	604.147	6.20	NIS 2
O V	629.730	5.93	NIS 2

Table 1. Lines observed with CDS and used in the analysis.

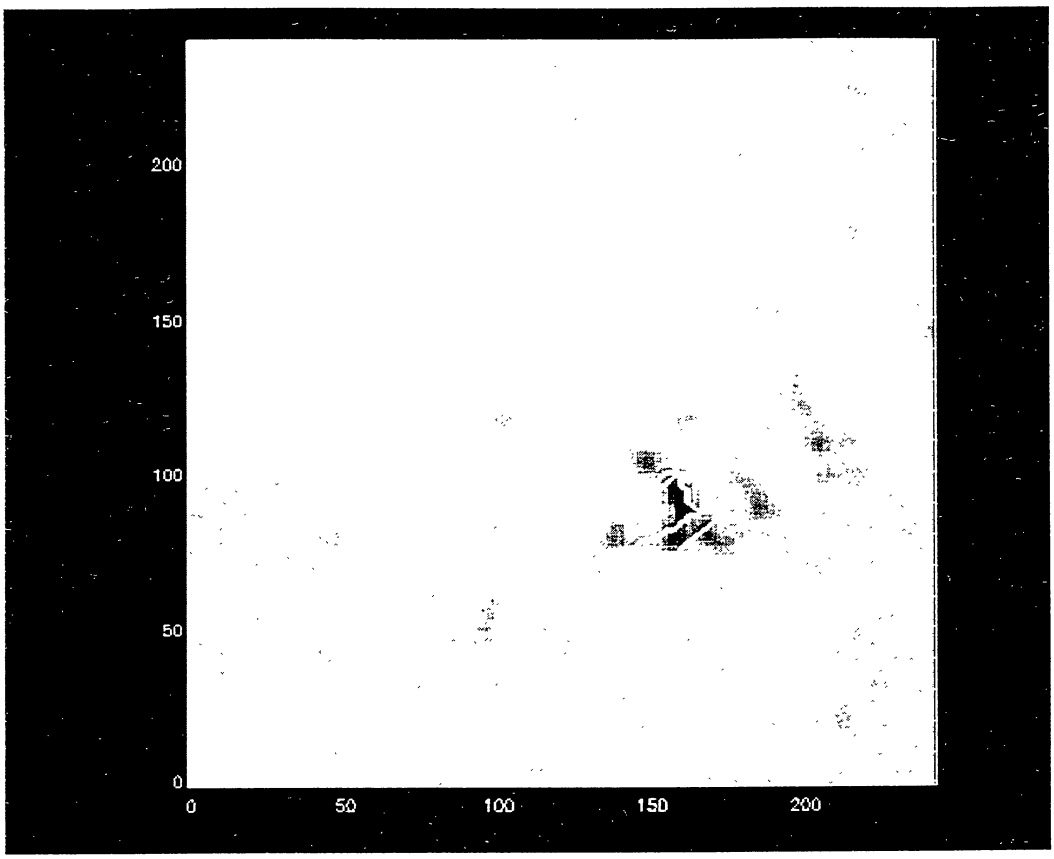

Figure 2. The magnetic field map of the region measured by MDI on SOHO with the adopted loop contours.

der to measure temperature and density along each structure. Emission from transition region lines (e.g. O V) are restricted to regions around the footpoints of the Fe XVI loops. Larger and fainter structures are visible in Mg IX lines, appearing completely uncorrelated with Fe XVI loops.

3.2. Density, temperature and pressure diagnostics

Density measurements for each section are performed by means of the intensity ratio of density sensitive pairs of lines. Lines of Fe XII (364.47 Å and 338.28 Å) and Fe XIII (359.64 Å +359.84 Å and 348.18 Å) have been used. Almost all density values are scattered within the experimental uncertainties around a constant value (Fig 3). Temperature measurements are performed through the Fe XVI/Fe XIV line ratio; temperatures slightly increase toward the loop center, and tend to decrease at the two feet. This is broadly consistent with loop models in the literature; however the changes are very small. The constant pressure assumption in loop models appears to be satisfied almost everywhere by the observations.

4. THE THEORETICAL MODEL AND DIAGNOSTIC TECHNIQUE

In this paper only basic charachteristics of the theoretical model are given, for further details we refer to Landini *et al.* (1999).

In stationary conditions and negligible velocity, a loop whose height is smaller than the gravitational scale height has constant pressure; for this reason in the present model we will assume that the pressure p_0 is constant, consistently with the line ratio measurements in Fig. 3.

The energy balance equation in the static approximation may be expressed as

$$E_r + E_i + E_c = 0 \qquad (1)$$

where E_r indicates radiative losses, E_i represents the (unknown) energy input and E_c indicates energy conduction by free electrons. The energy input is assumed to be constant with temperature.

In order to take the true radiative losses function properly into account a numerical integration of the energy balance equation has been performed using the radiative losses curve from Landi & Landini (1999). Radiative losses have been scaled according to

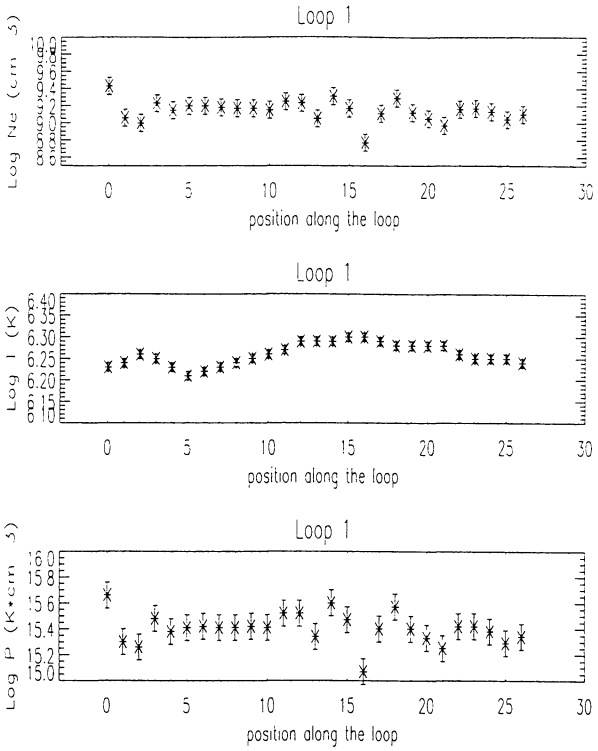

Figure 3. Plasma diagnostics for the outermost loop in Fig. 1.

$$E_{rad} = C\frac{p_0^2}{T^{5/2}}\varepsilon\left(\frac{T}{T_M}\right) \qquad C = 2\times 10^{12} \qquad (2)$$

where T_M is the temperature at which the energy input balances the radiative losses and where conductive energy vanishes, and $\varepsilon\left(\frac{T}{T_M}\right)$ are the scaled radiative losses. The constant loop section assumption commonly adopted in literature is released, and a variable loop section has been adopted. The geometrical cross-section of the loop (S) has been parametrized with

$$S = S_m + (S_M - S_m)\times(tanh\theta)^w \quad \Rightarrow \quad S = S_M\,\sigma(\theta) \qquad (3)$$

where $\theta = nt$, with $t = \frac{T}{T_M}$ scaled temperature, and S_M and S_m are the maximum and minimum loop section respectively. The w value is chosen as the one providing the best agreement between theoretical and observed line intensities. The variable loop section assumption is supported by the observations: the image of the loop in a transition region line is completely different from that of a coronal line since radiation originates in the loop's feet and in general the emitting region appears much smaller than the coronal loop section.

This model allows to determine all the loop plasma parameters; in particular the loop length is given by

$$L_{loop} = r(T_M)\sqrt{\frac{A}{C}}\frac{T_M^3}{p_0} \qquad A = 10^{-6} \qquad (4)$$

where $r(T_M)$ is a number near unity which is very weakly dependent on T_M. From this model theoretical line intensities may be computed. The intensity received on the Earth at distance d from the emitting loop in a line j is

$$I_j = \frac{S_M p_0}{4k^2}T_M\sqrt{\frac{A}{C}}\frac{1}{4\pi d^2}\int G_j(T)t^{1/2}f^{-1}\sigma^2(nt)dt \qquad (5)$$

where $G_j(T)$ is the Contribution Function of line j and f is the scaled conductive flux:

$$F_{cond} = f\sqrt{A\,C\,p_0^2\,T_M} \qquad (6)$$

The integral may be numerically evaluated for any value of T_M, the temperature where the energy losses equal the energy input. T_M is tied to the loop top temperature. We define the quantity

$$F(T_M) = \frac{I_j^o}{J_j(T_M)} \qquad (7)$$

where I_j^o is the observed line intensity and

$$J_j(T_M) = T_M\sum_i G_j(T_i)em\left(\frac{T_i}{T_M}\right) \qquad (8)$$

Considering Eq. 5, it is possible to show that if we plot all the $F(T_M)$ functions of all the observed lines versus T_M on the same plot, all the curves will meet in the point

$$\left(T_M, \frac{S_M p_0}{4k^2}\sqrt{\frac{A}{C}}\frac{1}{4\pi d^2}\right) \qquad (9)$$

Thus, it is possible to determine both the value of T_M (and hence the loop top temperature) and of $p_0 S_M$, which can be compared with observations.

5. COMPARISON WITH THE LOOP MODEL

The method described in Sect. 4. has been applied to line intensities emitted by the loops: these have been measured from spectra averaged on segments of the loop regions displayed in Fig. 1. The results are shown in Fig. 4 for the innermost loop in Fig. 1.

Each curve displays the scaled values of $p_0 \times S_M$ versus T_M that fits each observed line emission, calculated using Eq. 7. The region of the plot where all the curves meet together allows to estimate $p_0 \times S_M$ and

T_M values that satisfy all the observations. When T_M is known the measured loop length constrains p_0 and this allows to evaluate S_M and compare it with the measured loop width.

The physical parameters obtained from the model are reported in Table 2; along with the model predictions also the loop pressures and lengths as determined from observations are reported for comparison. Several comments are needed.

Table 2 shows that the considered loops have a very similar top temperature and pressure values, while their length and section radius R are slightly different. Also the parameters determining the shape of each loop change.

There is an excellent agreement between the measured and predicted loop pressure, while predicted top temperatures are always higher than the measured values by less than 20%. Also the predicted and measured cross-section radius R show agreement within the errorbars, although the predicted value is slightly higher than the observed one.

The loop shape parameters allow to determine the loop section at transition region temperatures, whose dimension are smaller than the pixel size: this explains why loop footpoints are not clearly visible at low temperatures. Model section versus temperature is shown in Fig. 6.

The temperature versus loop length model is displayed in Fig. 5, while Fig. 7 shows the conductive flux as a function of temperature.

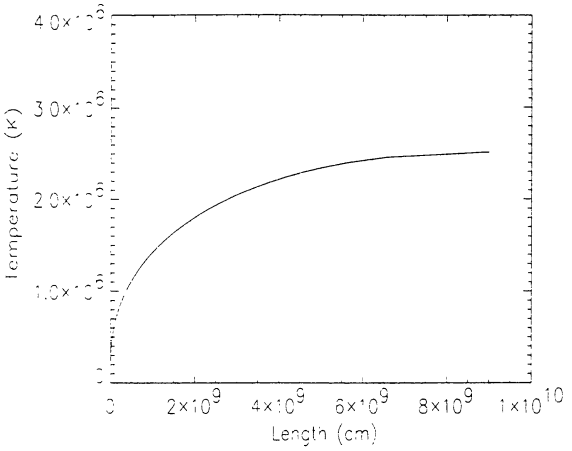

Figure 5. Temperature versus position along the loop model.

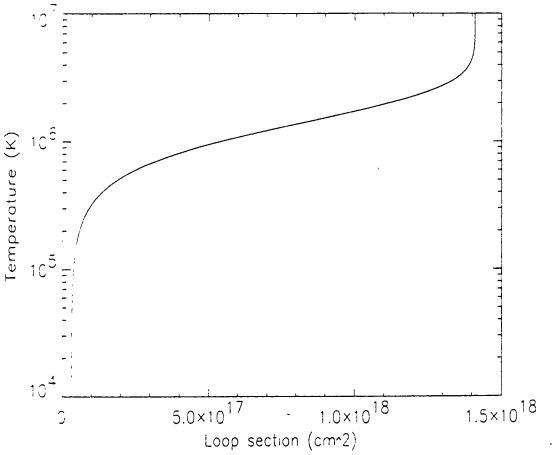

Figure 6. Model cross-section for the outermost loop in Fig. 1 as a function of temperature.

6. CONCLUSIONS

In the present work CDS, EIT and MDI observations (JOP 54) of active region loops are analyzed. The physical properties of the emitting plasma along the loop length have been determined and their values have been compared with an improved theoretical model derived from that of Landini & Monsignori Fossi (1975). The model allows to determine all the loop plasma parameters and also the shape of the loop itself. It has been shown that in order to have agreement with transition region lines it is necessary to assume a variable loop section. The temperature and pressure values for the model are compared with the values derived from observations and a good agreement is found; theoretical loop top temperatures from the model slightly exceed the experimental values from line ratios. Agreement is found also between theoretical and experimental loop section radius.

REFERENCES

Dere, K.P., Landi, E., Mason, H.E., Monsignori Fossi, B.C., Young, P.R., 1997, A&AS, 125, 149

Harrison, R.A., et al., 1995, Solar Physics, 162, 233

Landi, E., Landini, M., Dere, K.P., Young, P.R., Mason, H.E., 1999, A&AS, 135, 339

Landi, E., Landini, M., 1999, A&A, in press

Landini. M., Monsignori Fossi, B.C.,1973, A&A, 25, 9

Landini. M., Monsignori Fossi, B.C.,1975, A&A, 42, 213

Landini. M., Brković, A., Landi, E., Rüedi, I., Solanki, S., 1999, A&A, in preparation

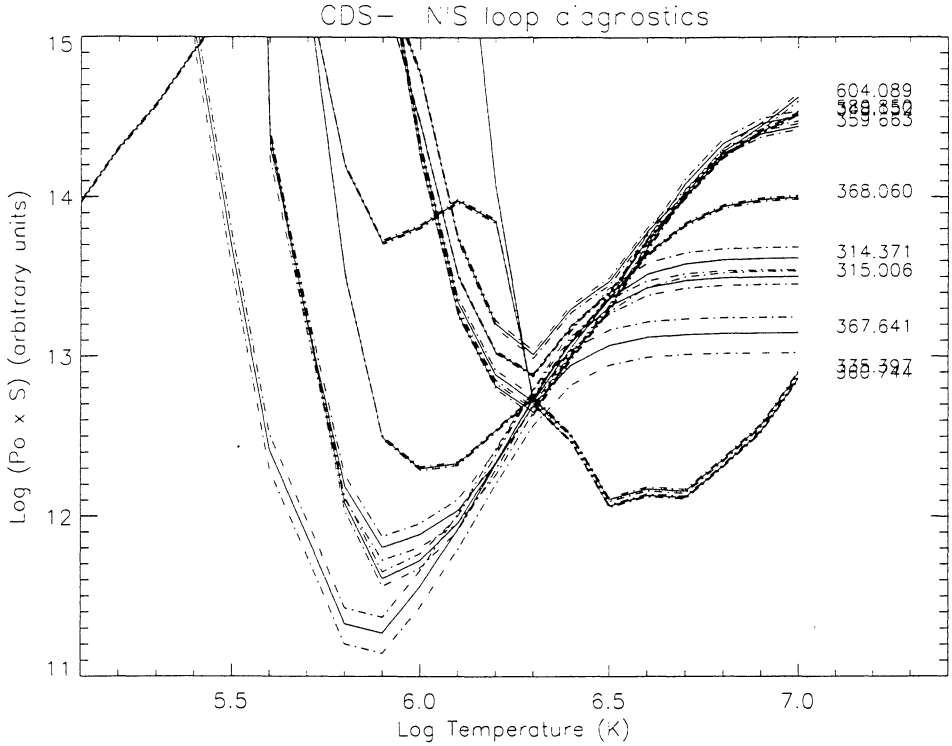

Figure 4. Values of $p_0 S$ as a function of temperature T_M for each spectral line for loop 3.

Loop	$\frac{S_M}{S_m}$	p_0^{meas}	p_0^{th}	Log T_{max}^{meas}	Log T_{max}^{th}	L^{meas}	R^{th}	R^{meas}
1	45	0.78±0.28	0.73±0.22	6.30±0.03	6.36±0.03	$(1.69 \pm 0.15) \times 10^5$	9400±3700	6706±1500
2	25	0.85±0.25	0.79±0.19	6.29±0.03	6.36±0.03	$(1.56 \pm 0.14) \times 10^5$	8500±3400	6235±1500
3	80	0.87±0.27	0.98±0.32	6.27±0.03	6.36±0.03	$(1.25 \pm 0.15) \times 10^5$	9000±4000	6524±1500

Table 2. Comparison between the physical properties of the observed loops measured from observations and determined by the theoretical model. R and L values are in km, p_0 is in dyne cm^{-2}, T in K.

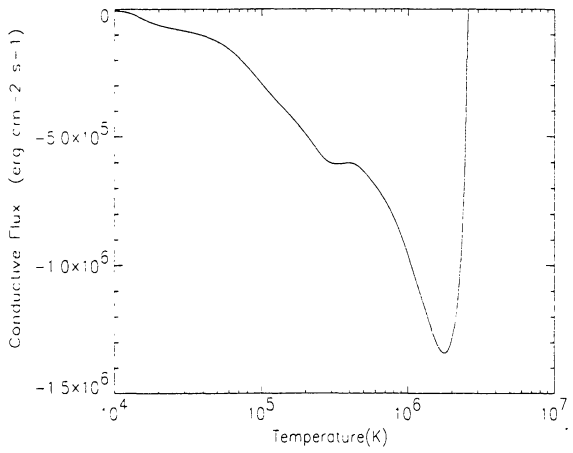

Figure 7. Conductive flux versus temperature.